

Carpal Tunnel Syndrome: Diagnosis with High-Resolution Sonography

Wolfgang Buchberger¹
 Werner Judmaier²
 Günther Birbamer³
 Manfred Lener²
 Christoph Schmidauer³

OBJECTIVE. Carpal tunnel syndrome is characterized by typical anatomic changes that can be shown with high-resolution sonography. To determine whether these findings are reliable and can be used to establish the diagnosis, sonograms of patients with the disease were compared with sonograms obtained in patients with normal wrists. Also compared were sonograms and MR images obtained in the patients with carpal tunnel syndrome.

SUBJECTS AND METHODS. Twenty wrists in 18 consecutive patients with clinical symptoms of carpal tunnel syndrome and with abnormal nerve conduction studies were examined with real-time sonography and MR imaging. The sonograms and MR images were evaluated quantitatively by two unbiased observers with regard to the size and shape of the median nerve and the palmar bowing of the flexor retinaculum. A *t* test was used to compare these data with those from previous sonographic studies of 28 normal wrists. Correlation coefficients for the measurements obtained with sonography and with MR were calculated. The relative accuracies of different diagnostic criteria for the diagnosis of carpal tunnel syndrome were assessed by using receiver-operating-characteristic analytical techniques.

RESULTS. Characteristic findings on both MR and CT scans of the 20 wrists with carpal tunnel syndrome included swelling of the median nerve in the proximal part of the carpal tunnel in 16 wrists, flattening of the median nerve in the distal part of the carpal tunnel in 13 wrists, and increased palmar bowing of the flexor retinaculum in nine wrists. Comparison with the data of 28 normal wrists proved that these findings were significant ($p < .01$ to $p < .001$). Receiver-operating-characteristic analysis showed that the discrimination between wrists in normal subjects and in patients with carpal tunnel syndrome achieved with each of the three diagnostic criteria was not significantly different. Measurements of the size and flattening of the median nerve obtained from sonograms were similar to those on MR images, whereas sonography was less accurate for measuring the palmar bowing of the flexor retinaculum.

CONCLUSION. We conclude that the results of sonography are reliable, and that the diagnosis of carpal tunnel syndrome can be established on the basis of sonographic findings.

AJR 159:793-798, October 1992

Received January 29, 1992; accepted after revision April 30, 1992.

¹ Department of Radiology, University of Innsbruck, Anichstrasse 35, A-6020 Innsbruck, Austria. Address reprint requests to W. Buchberger.

² Institute of Magnetic Resonance Imaging and Spectroscopy, University of Innsbruck, A-6020 Innsbruck, Austria.

³ Department of Neurology, University of Innsbruck, A-6020 Innsbruck, Austria.

0361-803X/92/1594-0793
 © American Roentgen Ray Society

Differentiation between carpal tunnel syndrome and other nerve entrapments, such as cervical root compression, thoracic outlet syndrome, or nerve entrapment in the forearm (anterior interosseous nerve syndrome), is not always possible on the basis of clinical findings alone, and the results of nerve conduction studies also may be equivocal [1, 2]. In addition, selecting treatment requires more precise information about the extent and cause of median nerve compression.

MR imaging has been used successfully for evaluating the carpal tunnel [3-5]. However, its high cost and time requirement limit its application for routine clinical use. In a preliminary study, 28 normal wrists and 28 wrists in patients with surgically proved carpal tunnel syndrome were examined with high-resolution sonography [6]. Quantitative analysis of the cross-sectional area and shape of the median nerve

and of the palmar bowing of the flexor retinaculum provided information that was used to define objective criteria for the diagnosis of carpal tunnel syndrome. The present study was undertaken to determine whether these findings are reliable and can be used to establish the diagnosis and to determine the accuracy of measurements obtained on sonograms by using MR as the gold standard.

Subjects and Methods

Twenty wrists of 18 consecutive patients with carpal tunnel syndrome were studied. The 14 women and four men in this group were 23–82 years old (mean, 57 years). The right wrist was affected in nine cases and the left wrist in seven cases; two patients had bilateral carpal tunnel syndrome. All patients had pain and sensory impairment in the distribution of the median nerve, and 10 patients had paresis of the abductor pollicis brevis. Electrodiagnostic studies were done in all patients. The motor latency of the median nerve was prolonged in all wrists, and the sensory latency was abnormal in seven. In 13 wrists, no action potential could be evoked on stimulation of the afferent fibers of the median nerve.

Sonography was performed with real-time equipment (Picker LSC 9500, Hitachi Medical Corp., Tokyo, Japan) and a 7.5-MHz linear probe with a standoff. Axial images at the distal radioulnar joint, the pisiform bone, and the hook of the hamate bone and sagittal images of the flexor tendons and the median nerve were recorded with a multifram camera. At each level, the mediolateral and anteroposterior diameters of the median nerve were measured, and the cross-sectional area was calculated (it was assumed that the area had an elliptical shape). Flattening of the median nerve was calculated as the ratio of the nerve's major to its minor axis (flattening ratio). Bowing of the flexor retinaculum was determined by drawing a straight line between its attachments to the tubercle of the trapezium bone and the hook of the hamate bone and measuring the distance from this line to the palmar apex of the ligament (palmar displacement).

MR imaging was performed with a 1.5-T superconducting system (Magnetom, Siemens, Erlangen, Germany) and a surface coil. During imaging, the patients were prone, with the arm extended overhead and the palm placed on the surface coil. A 128 × 256 matrix, two repetitions, and a 15-cm field of view were used. The imaging protocol included axial T1-weighted (450–550/15 [TR/TE]), proton density-weighted (2400/15), and T2-weighted (2400/90) spin-echo images. In addition, coronal T1-weighted images were obtained in 16 patients and sagittal T1-weighted images were obtained in four. With both the T1- and T2-weighted sequences, the section thickness was 3–4 mm, with a 0.3-mm gap. Quantitative analysis was performed as described, without knowledge of the results of the sonographic examination. All measurements were done at the viewing console; built-in computer software was used.

Measurements obtained with sonography in 20 wrists of 18 patients with carpal tunnel syndrome were compared with those in 28 previously studied normal wrists [6]. The results of quantitative analysis in both groups were compared with a *t* test. Carpal tunnel syndrome was diagnosed when at least one of the following findings was shown: (1) increased cross-sectional area of the median nerve at the pisiform bone and/or at the hamate bone, (2) increased flattening ratio of the median nerve at the hamate bone, or (3) increased palmar displacement of the flexor retinaculum. Quantitative measurements of the cross-sectional area and the flattening ratio of the median nerve and of the palmar displacement of the flexor retinaculum were used to calculate true-positive and false-positive percentages at different critical values on a continuous scale. Receiver-operating-characteristic (ROC) curves were obtained by using

a maximum likelihood curve-fitting algorithm [7, 8]. Relative diagnostic accuracy was estimated for each single sonographic feature by using the individual area under the ROC curve [9].

Results

Sonography

In our earlier study [6] of 28 normal wrists, we found neither a significant increase in size nor flattening of the median nerve in the carpal tunnel (Fig. 1). The mean cross-sectional area of the median nerve was 7.9 mm² (range, 6.5–11.9 mm²; SD, 1.1 mm²) at the level of the distal radioulnar joint, 8.1 mm² (range, 6.7–12.8 mm²; SD, 1.3 mm²) at the pisiform bone, and 7.7 mm² (range, 6.3–11.6 mm²; SD, 1.1 mm²) at the hamate bone. The mean flattening ratio of the median nerve was 2.7 (range, 2.2–3.1; SD, 0.3) at the distal radioulnar joint, 3.0 (range, 1.7–4.0; SD, 0.5) at the pisiform bone, and 3.2 (range, 2.3–4.3; SD, 0.5) at the hamate bone. The mean palmar displacement of the flexor retinaculum was 2.1 mm (range, 0–3.1 mm; SD, 0.8 mm).

In the present study of 20 wrists in 18 patients with carpal tunnel syndrome, the mean cross-sectional area of the median nerve was 10.0 mm² (range, 7.2–14.8 mm²; SD, 2.0 mm²) at the distal radioulnar joint, 14.5 mm² (range, 8.8–20.5 mm²; SD, 3.8 mm²) at the pisiform bone, and 10.3 mm² (range, 5.9–15.9 mm²; SD, 2.5 mm²) at the hamate bone. As determined with the *t* test, the mean cross-sectional areas of the median nerve at the pisiform bone (*p* < .001) and at the hamate bone (*p* < .01) were significantly greater than in normal wrists. The mean flattening ratio was 2.7 (range, 2.2–3.1; SD, 0.4) at the level of the distal radioulnar joint, 2.7 (range, 2.0–3.7; SD, 0.4) at the pisiform bone, and 4.6 (range, 3.1–6.5; SD, 0.5) at the hamate bone. Compared with the normal wrists, the median nerve was significantly more flattened at the level of the hamate bone (*p* < .001). The palmar displacement of the flexor retinaculum (mean, 3.7 mm; range, 2.0–6.0 mm; SD, 1.1 mm) was significantly greater than in normal wrists (*p* < .001).

The normal range at two standard deviations of the cross-sectional area of the median nerve was calculated from the data obtained in normal wrists; it was 5.7–10.1 mm² at the level of the distal radioulnar joint, 5.5–10.7 mm² at the pisiform bone, and 5.5–9.9 mm² at the hamate bone. The normal range of the flattening ratio of the median nerve was 2.0–4.0 at the distal radioulnar joint and at the pisiform bone and 2.2–4.2 at the hamate bone. The normal range of the palmar displacement of the flexor retinaculum was 0.5–3.7 mm. Sixteen wrists showed swelling of the median nerve at the level of the pisiform bone (Fig. 2). In 11 cases, swelling of the median nerve also was seen at the level of the hamate bone. Thirteen wrists had increased flattening of the nerve at the level of the hamate bone, and nine wrists had increased palmar bowing of the flexor retinaculum (Fig. 3). The characteristic triad of median nerve swelling and flattening and increased bowing of the flexor retinaculum was seen in six wrists. Six other wrists showed median nerve swelling and flattening, and four others showed median nerve swelling and increased bowing of the flexor retinaculum. Swelling of the

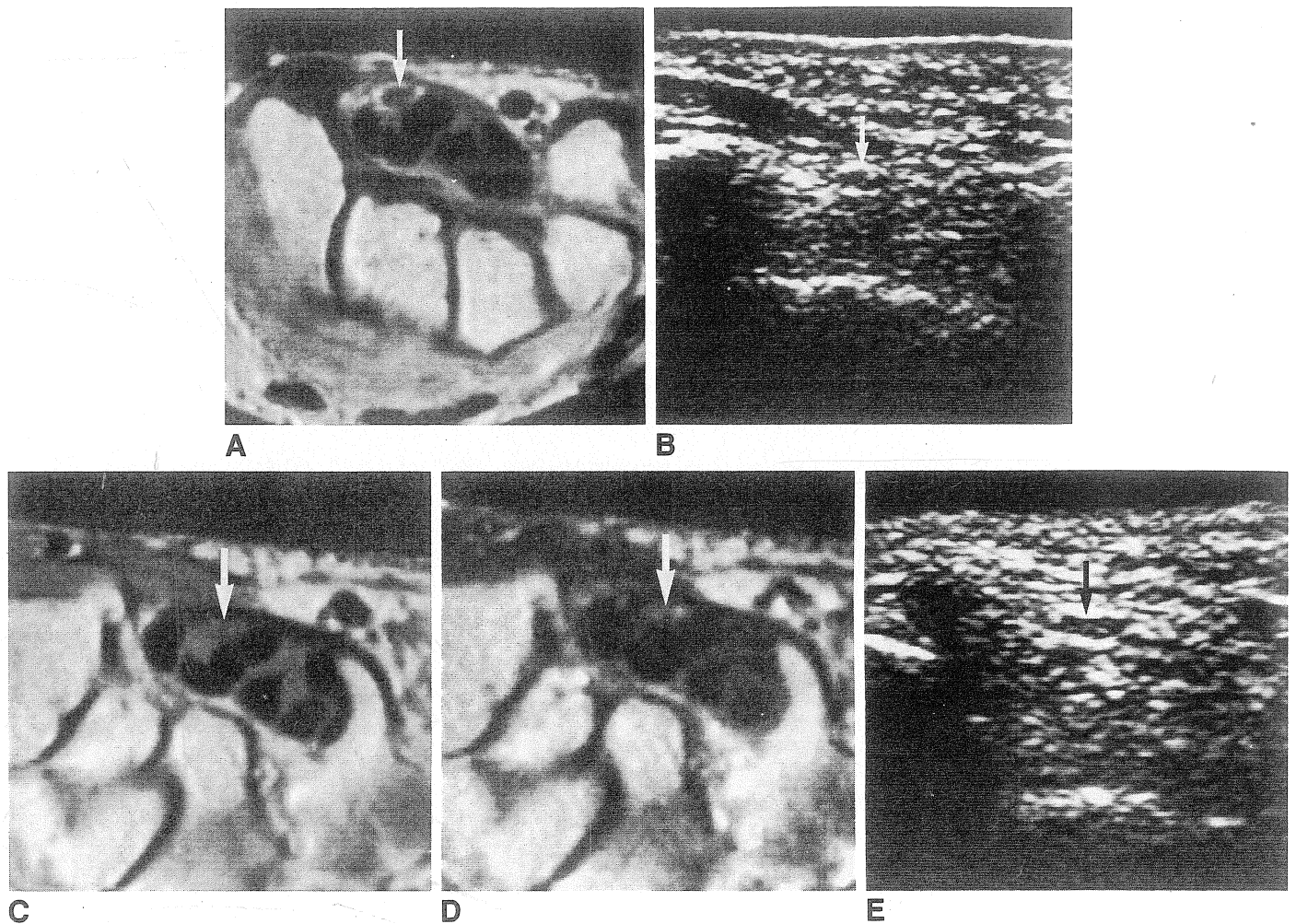


Fig. 1.—Normal carpal tunnel.

A, Axial T1-weighted (550/15) MR image of left wrist at pisiform bone shows median nerve (arrow) with normal size and shape.

B, Corresponding axial sonogram shows normal median nerve (arrow).

C, Axial T1-weighted (550/15) MR image at hamate bone shows normal median nerve (arrow). Only subtle flattening is seen compared with shape of nerve at pisiform bone.

D, T2-weighted (2400/90) MR image at same level shows no significant increase in signal intensity of median nerve (arrow).

E, Corresponding axial sonogram shows normal median nerve (arrow).

median nerve was the only finding in two wrists, and increased flattening of the median nerve was the only finding in one. In one wrist, the sonographic findings were normal despite clinical and electrodiagnostic evidence of carpal tunnel syndrome. The ROC curves for the cross-sectional area and the flattening ratio of the median nerve and for the palmar displacement of the flexor retinaculum are displayed in Figure 4. The individual area under the ROC curve was 0.90 for the flattening ratio, 0.86 for the swelling ratio, and 0.85 for the palmar displacement; the differences were not statistically significant.

In five wrists, the flexor tendons were separated by an unusual amount of hypoechoic tissue, probably representing proliferated synovium of the flexor tendon sheaths (Fig. 2D). In one wrist, a 10-mm anechoic structure with smooth contours was seen deep to the flexor tendons, probably representing a ganglionic cyst.

MR Imaging

In all 20 wrists, the signal intensity of the median nerve was increased on both proton density-weighted and T2-weighted images (Figs. 2C, 3B, and 5). The increased signal was more obvious on T2-weighted images and extended from the entrance of the carpal tunnel to as far distally as the metacarpal bases.

Swelling and flattening of the median nerve and increased palmar bowing of the flexor retinaculum were visualized equally as well on MR images as on sonograms (Figs. 2 and 3). Measurements of the cross-sectional area and of the flattening ratio of the median nerve on MR images were similar to those obtained with sonograms (Figs. 6A and 6B). The differences were not statistically significant ($p < .01$ to $p < .001$). Measurements of palmar displacement of the flexor retinaculum correlated less well ($p < .05$) (Fig. 6C).

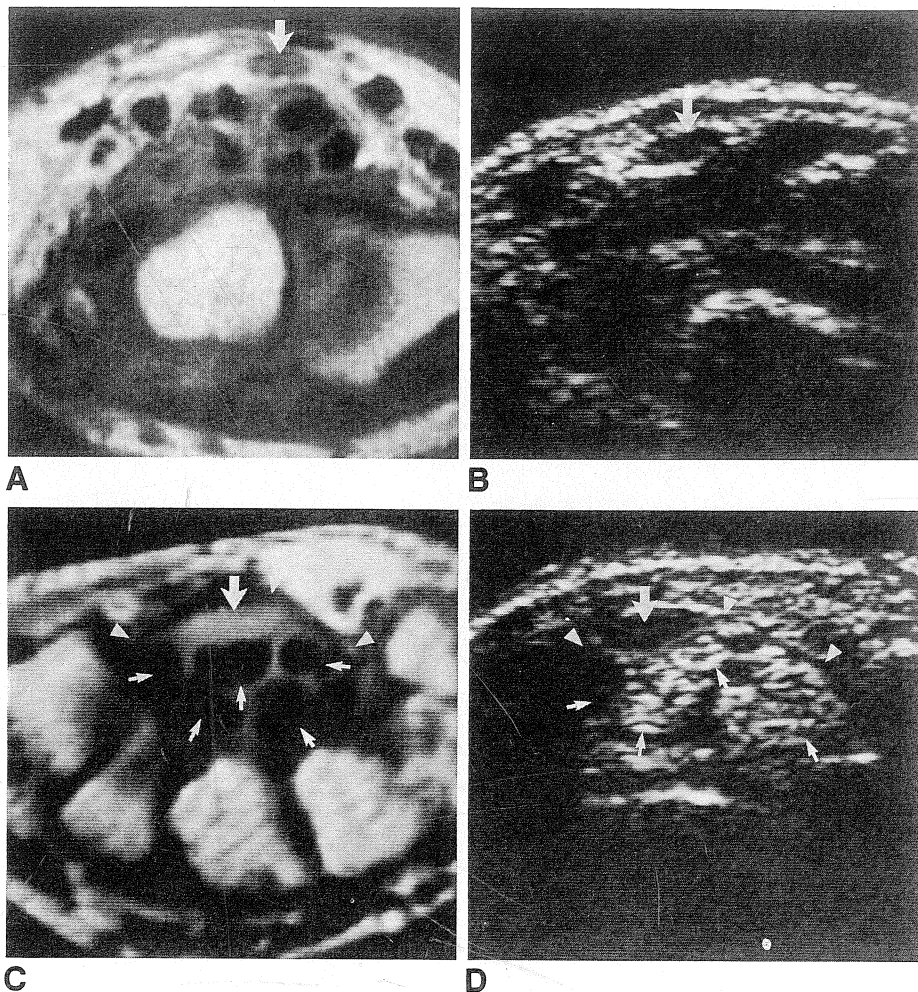


Fig. 2.—43-year-old woman with carpal tunnel syndrome.

A, Axial T1-weighted (450/15) MR image of left wrist at distal radioulnar joint shows normal size and shape of median nerve (arrow).

B, Corresponding axial sonogram shows normal median nerve (arrow).

C, Axial proton density-weighted (2400/15) MR image at pisiform bone shows enlarged median nerve (large arrow) with increased signal intensity. Note increased separation of flexor tendons (small arrows) by moderately thickened tendon sheaths and palmar bowing of flexor retinaculum (arrowheads).

D, Corresponding axial sonogram shows enlarged median nerve (large arrow) and unusual amount of hypoechoic tissue between flexor tendons (small arrows). Note significant bowing of flexor retinaculum (arrowheads).

In eight wrists, MR imaging showed obvious thickening of the flexor tendon sheaths (Fig. 2C). The signal intensity of the synovium was increased on T2-weighted images (Fig. 3B). In three wrists, the tendons had poorly defined margins, suggesting edema. Ganglionic cysts 4–10 mm in diameter were seen in another three wrists (Fig. 5).

Discussion

Because of its inherently high contrast, which allows accurate depiction of the soft-tissue structures of the hand, MR imaging has been the only imaging technique of diagnostic value in carpal tunnel syndrome. Middleton et al. [3] and Mesgarzadeh et al. [4, 5] described the normal anatomy of the carpal tunnel, as shown with MR imaging, and reported on preliminary observations in patients with carpal tunnel syndrome. Real-time high-frequency sonography has been used to diagnose soft-tissue lesions of the hand [10, 11]. The sonographic appearance of various peripheral nerves of the extremities, including the median nerve, has been described by Fornage [12]. Calleja Cancho et al. [13] described the normal anatomy of the carpal tunnel, seen on sonograms, and discussed the ability of sonography to show the median nerve on sagittal and axial scans. We found earlier that

sonography can be used to detect anatomic changes in patients with carpal tunnel syndrome [6]. Consistent with the results of Mesgarzadeh et al. [5], our findings showed that, regardless of the cause, carpal tunnel syndrome included swelling of the median nerve at the entrance and in the proximal part of the carpal tunnel, flattening of the median nerve in the distal part of the carpal tunnel, and increased bowing of the flexor retinaculum.

In the present study, at least one of these diagnostic changes was shown in all wrists except one. Diffuse or localized swelling and increased flattening of the median nerve were the most common findings. Both observations are well described in the surgical literature. Rietz and Örne [2] found swelling of the median nerve in 66% of cases. Phalen [14] observed bulbous swelling of the median nerve (pseudoneuroma) in 45 of 212 wrists operated on and flattening of the median nerve beneath the flexor retinaculum in 151 of 212. Increased bowing of the flexor retinaculum was seen less frequently, and usually was associated with swelling of the median nerve.

Enlargement and flattening of the median nerve may be evident at subjective evaluation. However, in most cases, quantitative studies are necessary. The accuracy of sonographic measurements is limited by the axial and lateral

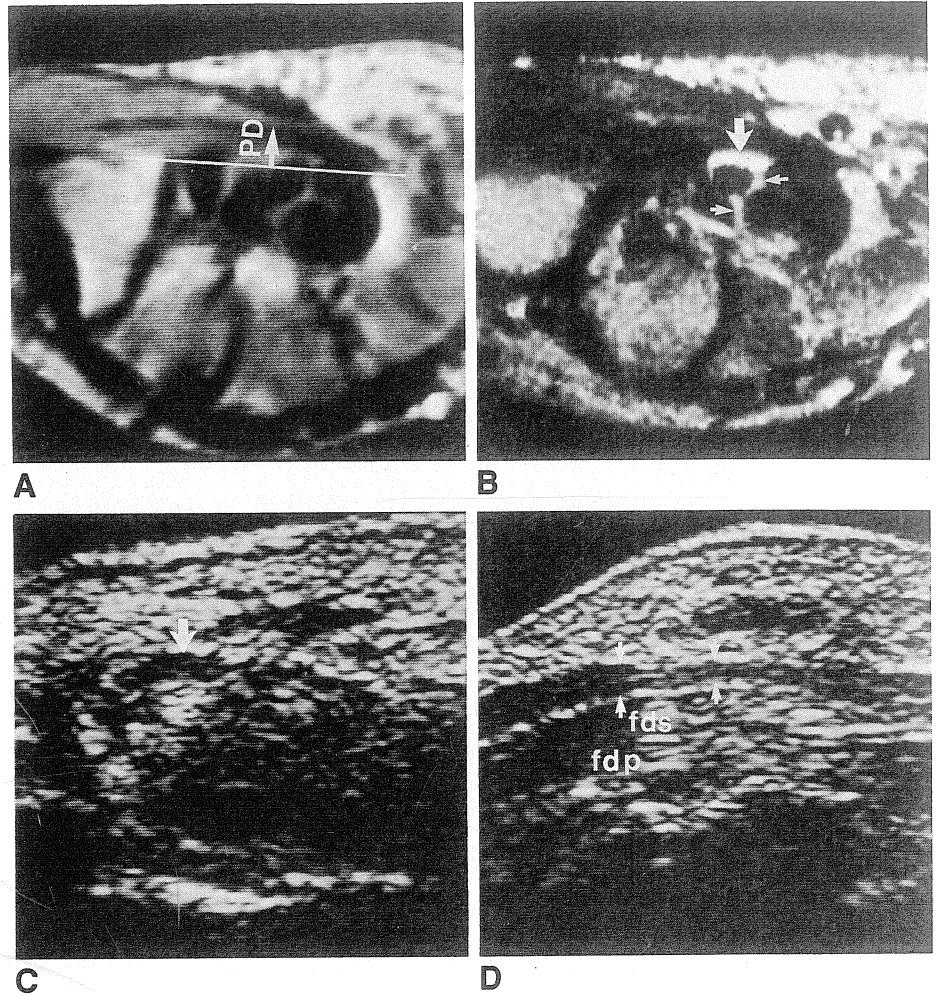
Fig. 3.—51-year-old woman with carpal tunnel syndrome.

A, Axial T1-weighted (450/15) MR image of left wrist at hook of hamate bone shows increased palmar bowing of flexor retinaculum. PD = palmar displacement.

B, Corresponding axial T2-weighted (2400/90) MR image shows increased signal of flattened median nerve (large arrow). Thickening and increased signal intensity of flexor tendon sheaths (small arrows) suggest synovitis.

C, Corresponding axial sonogram shows flattened median nerve (arrow).

D, Sagittal sonogram shows flattening of median nerve (arrows) in distal part of carpal tunnel. Tendons of flexor digitorum superficialis (fds) and profundus (fdp) are deep to median nerve.



resolution of the transducer, which, according to its manufacturer, is 0.2 mm for axial resolution and 0.5 mm for lateral resolution in the focal zone. In tissue, the effective spatial resolution depends on echo amplitude and tissue attenuation. In the carpal tunnel, the small differences in acoustic imped-

ance between the median nerve and its surroundings and the relatively high tissue attenuation result in a low signal-to-noise ratio. Despite these restrictions, the results of quantitative studies with sonography corresponded well with the results

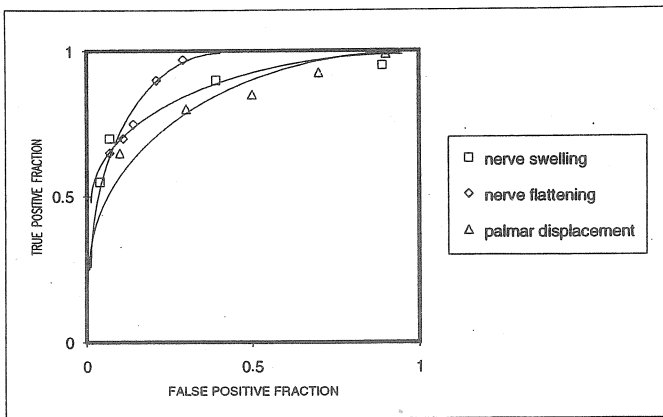


Fig. 4.—Graph shows receiver-operating-characteristic curves for different diagnostic criteria (swelling of median nerve, flattening of median nerve, and increased palmar displacement of flexor retinaculum).

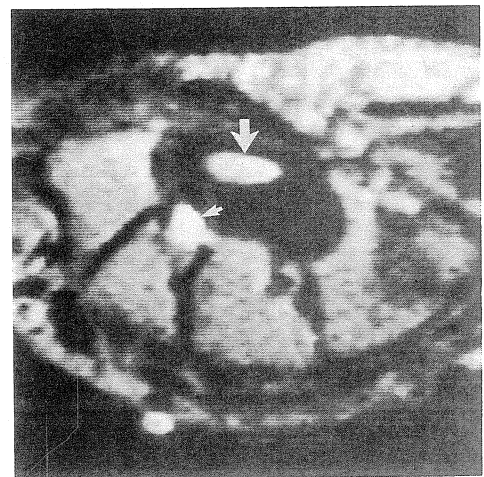


Fig. 5.—23-year-old woman with carpal tunnel syndrome. Axial T2-weighted (2400/90) MR image of right wrist at hook of hamate bone shows enlarged median nerve (large arrow) with increased signal intensity. Note high-signal-intensity ganglionic cyst (small arrow).

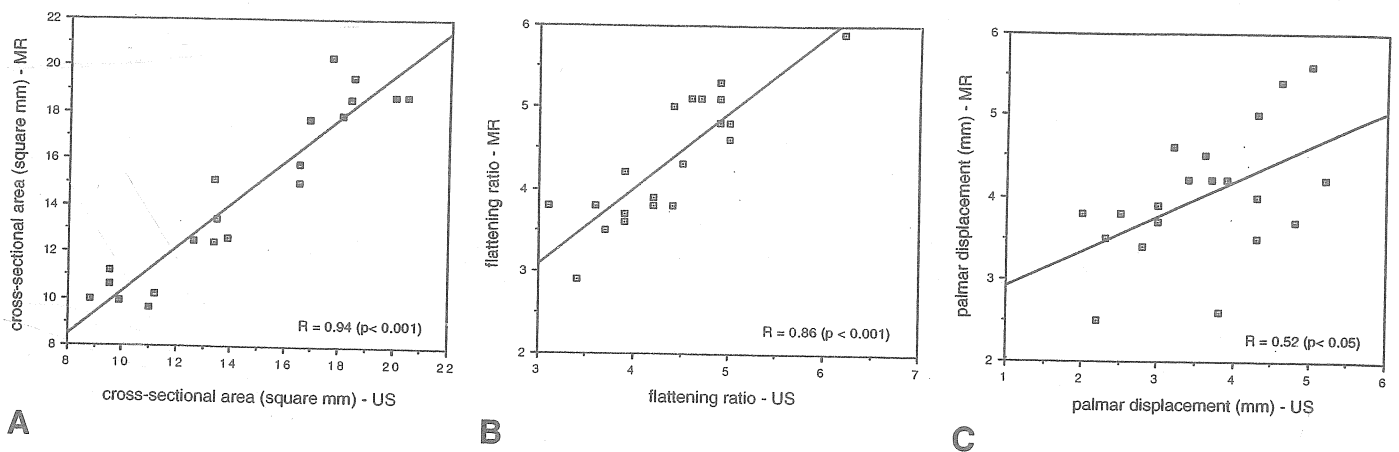


Fig. 6.—Graphs of measurements obtained from sonograms (US) and MR images in 20 wrists with carpal tunnel syndrome.
 A, Cross-sectional area of median nerve at level of pisiform bone.
 B, Flattening ratio of median nerve at level of hamate bone.
 C, Palmar displacement of flexor retinaculum.

of similar studies with MR imaging. Measurements of the cross-sectional area and of the flattening ratio of the median nerve were not significantly different with the two imaging techniques. Measurements of the palmar bowing of the flexor retinaculum were less accurate with sonography than with MR imaging. This was probably due to poor visualization of the carpal bones on sonograms, which made identification of the measuring points difficult.

The diagnostic performance of a screening test is best evaluated by means of an ROC analysis [7, 8]. Although complete ROC analysis could not be performed in our study, the individual ROC curves for the cross-sectional area and the flattening ratio of the median nerve and for the palmar displacement of the flexor retinaculum, obtained with sonography, suggest that the discrimination ability of these measurements is sufficiently high to establish the diagnosis.

A comparison of the efficacy of sonography and MR imaging in the diagnosis of carpal tunnel syndrome was not the purpose of our study. However, our results suggest that, because of its excellent soft-tissue contrast, MR can show mild degrees of compression of the median nerve that may be missed on sonograms. In addition, the increased signal intensity of the median nerve on proton density- and T2-weighted images, probably due to edema, is a frequent finding that facilitates the diagnosis [3, 5]. In our patients, MR imaging also was superior to sonography in the detection of etiologic findings, such as tendon-sheath thickening and ganglionic cysts. In summary, high-resolution real-time sonography has proved to be an effective method for diagnosing carpal tunnel syndrome. Its low cost, minimal time requirement, and general availability favor its use as the initial study in evaluating the carpal tunnel. The efficacy of sonography compared with MR

imaging and the complementary roles of the two techniques will require further evaluation.

REFERENCES

- Phalen GS. The carpal tunnel syndrome: seventeen years' experience in diagnosis and treatment of six hundred fifty-four hands. *J Bone Joint Surg [Am]* 1966;48-A:211-228
- Rietz KA, Ötne L. Analysis of sixty-five operated cases of carpal tunnel syndrome. *Eur J Surg* 1967;133:443-447
- Middleton WD, Kneeland JB, Kellman GM, et al. MR imaging of the carpal tunnel: normal anatomy and preliminary findings in the carpal tunnel syndrome. *AJR* 1987;148:307-316
- Mesgarzadeh M, Schneck CD, Bonakdarpour A. Carpal tunnel: MR imaging. Part I. Normal anatomy. *Radiology* 1989;171:743-748
- Mesgarzadeh M, Schneck CD, Bonakdarpour A, Amitabha M, Conway D. Carpal tunnel: MR imaging. Part II. Carpal tunnel syndrome. *Radiology* 1989;171:749-754
- Buchberger W, Schön G, Strasser K, Jungwirth W. High-resolution ultrasonography of the carpal tunnel. *J Ultrasound Med* 1991;10:531-537
- Metz CE. Basic principles of ROC analysis. *Semin Nucl Med* 1978;8:283-298
- Lusted LB. Decision-making studies in patient management. *N Engl J Med* 1971;284:416-424
- Hanley JA, McNeil BJ. The meaning and use of the area under a receiver operating characteristic (ROC) curve. *Radiology* 1982;143:29-36
- Fornage BD, Schernberg FL, Rifkin MD. Ultrasound examination of the hand. *Radiology* 1985;155:785-788
- Fornage BD, Rifkin MD. Ultrasound examination of the hand and foot. *Radiol Clin North Am* 1988;26:109-129
- Fornage BD. Peripheral nerves of the extremities: imaging with US. *Radiology* 1988;167:179-182
- Calleja Cancho E, Schawe-Calleja Cancho M, Milbradt H, Galanski M. Sonoanatomy and examination technique of the normal carpal tunnel (English abstr.). *Rofo Fortschr Geb Rontgenstr Neuen Bildgeb Verfahr* 1989;151:414-418
- Phalen GS. The carpal-tunnel syndrome: clinical evaluation of 598 hands. *Clin Orthop* 1972;83:29-40